

# Equivalence between exponential concentration in quantum machine learning kernels and barren plateaus in variational algorithms

Pranav Kairon,<sup>1,2</sup> Jonas Jäger,<sup>3,2</sup> and Roman V. Krems<sup>2,4</sup>

<sup>1</sup>*Department of Physics and Astronomy, University of British Columbia, Vancouver, B.C., Canada*<sup>a</sup>

<sup>2</sup>*Stewart Blusson Quantum Matter Institute, Vancouver, B.C., Canada*

<sup>3</sup>*Department of Computer Science and Institute of Applied Mathematics, University of British Columbia, Vancouver, B.C., Canada*

<sup>4</sup>*Department of Chemistry, University of British Columbia, Vancouver, B.C., Canada*<sup>†</sup>

(Dated: January 14, 2025)

We formalize a rigorous connection between barren plateaus (BP) in variational quantum algorithms and exponential concentration of quantum kernels for machine learning. Our results imply that recently proposed strategies to build BP-free quantum circuits can be utilized to construct useful quantum kernels for machine learning. This is illustrated by a numerical example employing a provably BP-free quantum neural network to construct kernel matrices for classification datasets of increasing dimensionality without exponential concentration.

## I. INTRODUCTION

Machine learning with quantum kernels [1–5] and variational quantum algorithms (VQAs) [6] are two distinct paradigms currently explored for computation with noisy quantum devices [7–11]. VQAs are restricted by barren plateaus (BPs) [12, 13]. BPs are regions in the variational parameter space where gradients of the cost function vanish exponentially with the number of qubits, leading to increasingly narrow gorges of optimal solutions [14]. This implies that an exponentially large number of measurements is required to estimate cost functions for VQAs with BP, as these estimates are otherwise dominated by the statistical measurement error (i.e., shot noise). The origin of BPs can be traced to the vanishing of inner products between quantum states in exponentially large Hilbert spaces. Exponential vanishing of inner products also hinders applications of quantum computing for estimating kernels for machine learning models [5, 15]. In kernel methods of machine learning, models are based on kernel matrices [15], which in quantum machine learning (QML), are estimated by measurements on a quantum computer [1–3]. Refs. [16, 17] show that both the expected value

<sup>a</sup> Currently at Department of Physics, University of Illinois at Urbana-Champaign, Urbana, IL 61801, USA

<sup>†</sup> rkrems@chem.ubc.ca

and variance of the off-diagonal elements of quantum kernel matrices decrease exponentially as the number of qubits used for building quantum kernels grows. This leads to exponential concentration (EC) of the kernel matrix around a diagonal matrix, implying that quantum kernels reduce to  $\delta$ -functions in a large Hilbert space and make quantum machine learning impractical.

Since BPs preclude the quantum advantage of VQAs [12], a significant focus of recent work has been on how to engineer quantum circuits for VQAs without BPs. It has been shown that BPs can be avoided by restricting the depth of quantum circuits [18], by building equivariance into the quantum ansatz [19], as well as by employing specific initialization strategies for variational optimization [20–24]. Previous work on how to prevent EC of quantum kernels is much more scarce. The proposed approaches include covariant quantum kernels [25], quantum kernel bandwidth methods [26], quantum Fisher kernels [27], and projected quantum kernel methods [28]. All these methods encode inductive bias into the quantum models, thereby restricting learning to a particular subspace of the Hilbert space. A rigorously proven relation between BPs in VQAs and concentration of kernel matrices is required to leverage and transfer results from the BP literature to quantum kernels.

It has been assumed that BPs and EC of quantum kernels are different manifestations of the same problem [13, 17, 29–32]. However, to the best of our knowledge, no rigorous proof of the connection, or limitations thereof, between BPs in VQAs and EC in quantum kernels has been presented. Here, we formalize the relation between BPs in VQAs and EC of quantum kernels by transferring training bounds derived for VQAs to QML using quantum kernels. There are two possible implications of BPs for quantum kernels. First, training a machine learning model with parametrized kernels, which entails an optimization of kernel parameters, can be directly formulated as a variational problem [3, 33]. This optimization problem may suffer from BPs [17]. The second implication is EC of quantum kernels. In order to separate these two problems, we consider fixed, non-parametric quantum kernels and examine the effect of BP, or lack thereof, on learning with quantum kernels constructed from the quantum circuits employed for VQA or quantum neural networks.

Schuld *et al.* [4] established connections between quantum kernel methods and VQAs. Here, we use a similar approach to prove that the upper and lower bounds on the cost function for the variational problems transfer to the bounds on estimation of the matrix elements of the corresponding quantum kernel. In particular, we show that if an ansatz leads to BP-free VQAs with a global observable [34], then there exists a quantum kernel that does not suffer from EC. We formalize the connection between BP, or their absence, in variational algorithms and EC of quantum kernels by formulating a bound transfer theorem. The proof of the theorem is aided by two lemmas introduced

to examine how concentration of kernel functions of data is related to concentration of functions of parameters.

## II. DEFINITIONS

For a supervised learning task, the dataset is given by  $\mathcal{D} := (\mathbf{x}_i, \mathbf{y}_i)_{i=1}^{N_s}$ , where  $\mathbf{x}_i \in \mathcal{X}$  are input vectors,  $\mathbf{y}_i \in \mathcal{Y}$  are the labels and  $N_s$  is the number of data points. The inputs are related to the labels via a black box function  $f : \mathcal{X} \rightarrow \mathcal{Y}$ , and the task is to determine a QML model  $h_{\boldsymbol{\theta}}$  parameterized by  $\boldsymbol{\theta}$  such that  $h_{\boldsymbol{\theta}} : \mathcal{X} \rightarrow \mathcal{Y}$  approximates  $f$ . Note that this work focuses on classical data, i.e. the inputs and outputs are both classical [35].

### A. Exponential concentration of quantum kernels

We consider an  $n$ -qubit system, and a quantum feature map  $\phi$ , that encodes  $\mathbf{x}_i$  into a quantum state in an  $n$ -qubit Hilbert space, associated with the pure density matrix  $\rho(\mathbf{x}_i) = |\phi(\mathbf{x}_i)\rangle\langle\phi(\mathbf{x}_i)|$ . The feature map  $\phi$  can be implemented through a unitary quantum circuit  $U(\mathbf{x})$  acting on a common initial state  $\rho_0$ . The data embedding  $U(\mathbf{x})$  acts as a generator of a unitary ensemble, defined over all possible input data vectors  $\mathbf{x}_i \in \mathcal{X}$ . From a functional analysis perspective, we have that  $U : \mathcal{X} \rightarrow \mathbb{U}_x \subseteq \mathcal{U}(2^n)$ , where  $\mathcal{U}(2^n)$  is the total space of unitaries and  $\mathbb{U}_x = \{U(\mathbf{x}) | \mathbf{x} \in \mathcal{X}\}$ . The density matrices are supported on the  $2^n$ -dimensional Hilbert space  $\mathcal{H}$ , where the inner product is defined as  $\langle \rho | \rho' \rangle_{\mathcal{H}} = \text{Tr}(\rho \rho')$ , i.e., the Hilbert-Schmidt inner product. An inner product of quantum states in  $\mathcal{H}$  can be used to define a kernel function  $\kappa(\mathbf{x}, \mathbf{x}')$  of a reproducing kernel Hilbert space,

$$\kappa(\mathbf{x}, \mathbf{x}') = |\langle \phi(\mathbf{x}) | \phi(\mathbf{x}') \rangle|^2 = |\langle 0^{\otimes n} | U^\dagger(\mathbf{x}) U(\mathbf{x}') | 0^{\otimes n} \rangle|^2 = \text{Tr}(\rho(\mathbf{x}) \rho(\mathbf{x}')) \quad (1)$$

where  $\rho(\mathbf{x}) = U(\mathbf{x}) \rho_0 U^\dagger(\mathbf{x})$  and  $\rho(\mathbf{x}') = U(\mathbf{x}') \rho_0 U^\dagger(\mathbf{x}')$  are the density matrices corresponding to the quantum states representing the data points  $\mathbf{x}$  and  $\mathbf{x}'$  [5, 15], and  $\rho_0 = |0\rangle\langle 0|^{\otimes n}$ . The sequence  $U^\dagger(\mathbf{x}) U(\mathbf{x}')$  in Eq. (1) can be used to implement a kernel on a quantum computer, as illustrated by the diagram of the quantum circuit used to evaluate kernel entries in Fig. 1.

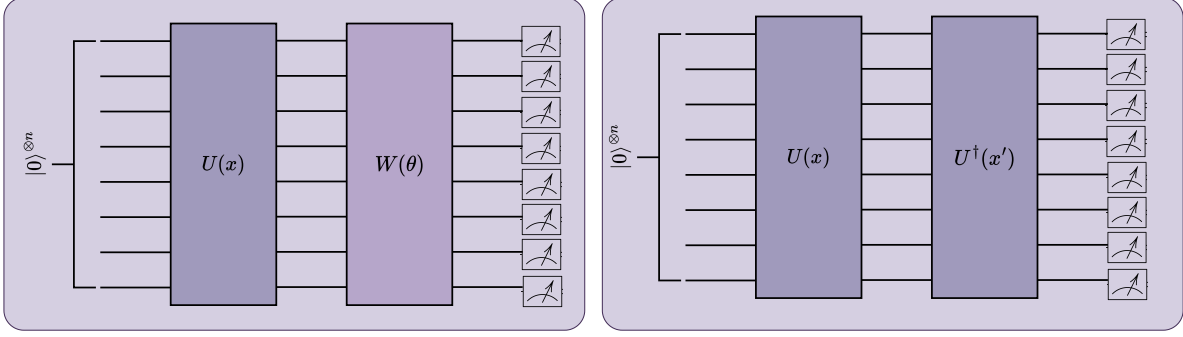


Figure 1. Schematic quantum circuit for a QNN (left) and a quantum kernel (right). The final output is the expectation value of  $|0\rangle\langle 0|^{\otimes n}$ .

EC of quantum kernels is defined as follows.

**Definition 1. (Deterministic)** Deterministic exponential concentration of quantum kernel  $\kappa(\mathbf{x}, \mathbf{x}')$  in the number of qubits  $n$  is defined as

$$|\kappa(\mathbf{x}, \mathbf{x}') - \mu| \leq \beta, \quad \beta \in O(1/b^n) \quad (2)$$

$$\mu = \mathbb{E}_{\mathbf{x}, \mathbf{x}'}[\kappa(\mathbf{x}, \mathbf{x}')] \quad (3)$$

for some  $b > 1$  and all pairs of data points  $\mathbf{x}, \mathbf{x}'$ .

**Definition 2. (Probabilistic)** Probabilistic exponential concentration of quantum kernel  $\kappa(\mathbf{x}, \mathbf{x}')$  is defined as follows:

$$\Pr_{\mathbf{x}, \mathbf{x}'}[|\kappa(\mathbf{x}, \mathbf{x}') - \mu| \geq \delta] \leq \frac{\beta^2}{\delta^2}, \quad \beta \in O(1/b^n). \quad (4)$$

That is, the probability that  $\kappa(\mathbf{x}, \mathbf{x}')$  deviates from  $\mu$  by a small amount  $\delta > 0$  becomes exponentially small for all  $\mathbf{x}, \mathbf{x}'$  as the number of qubits  $n$  grows. Here we have made use of Chebyshev's inequality:

$$\Pr(|\kappa(\mathbf{x}, \mathbf{x}') - \mu| \geq \delta) \leq \frac{\text{Var}_{\mathbf{x}, \mathbf{x}'}[\kappa(\mathbf{x}, \mathbf{x}')] }{\delta^2}. \quad (5)$$

Note that probabilistic kernel concentration is more general than the deterministic case since any kernel that concentrates deterministically is also probabilistically concentrated, but the reverse is generally not true.

EC can also be observed in the eigenspectrum of the kernel matrix. The framework proposed in Ref. [36] considers the number of samples necessary for a model to learn a target function. The learning requirement for each eigenmode of the kernel function is determined by the corresponding eigenvalue of the kernel matrix. Consequently, a “flat” eigenspectrum indicates a requirement of an

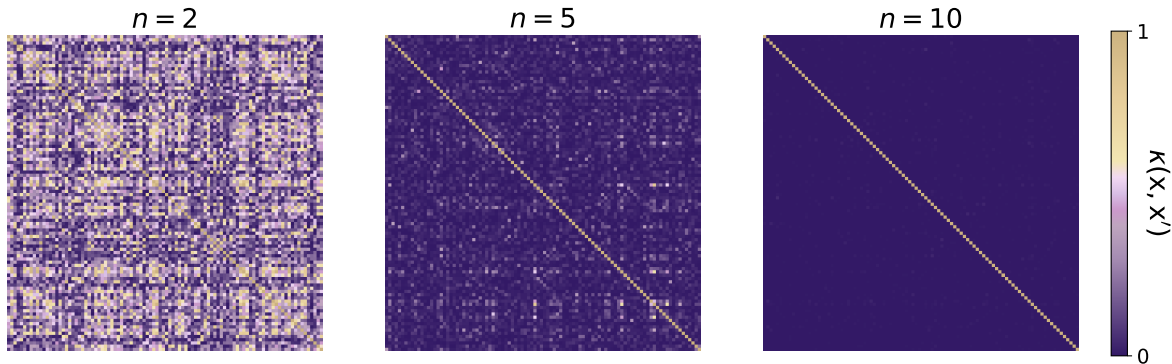


Figure 2. Exponential concentration of a quantum kernel: comparison of the kernel matrices constructed using an ansatz proposed by Havlíček *et al.* [15] for binary classification on MNIST dataset [37]. The matrices are constructed for 100 data points with the number of dimensions reduced to the corresponding number of qubits by principal component analysis. Each dimension is encoded into a single independent qubit. The kernel matrices shown are for qubit numbers  $n = 2, 5, 10$ .

exponentially large amount of data to learn each eigenmode, which leads to a high generalization error for kernel modes trained with a finite number of samples.

Fig. 2 presents a numerical demonstration of exponential concentration. For this example, we compute the kernel matrices with the data based on the modified National Institute of Standards and Technology (MNIST) resources, including handwritten digit images [37]. The matrices are constructed for 100 data points with the number of dimensions reduced to the corresponding number of qubits by principal component analysis (PCA). Each PCA-reduced dimension is encoded into a single independent qubit. Fig. 2 shows the kernel matrices thus constructed for qubit numbers  $n = 2, 5$ , and 10. It can be seen that the off-diagonal elements of the kernel matrix quickly decay and vanish for  $n = 10$ . This result is compared in a subsequent section with the kernel matrices obtained from a quantum algorithm, which is known to be BP-free.

## B. Barren plateaus in variational methods

The present work establishes the connection between EC of quantum kernels and BPs through properties of the cost function of VQAs, in general, and quantum neural networks (QNNs), in particular. Parameterized state evolutions, realized through parameterized quantum circuits  $W(\boldsymbol{\theta})$ , are at the core of VQAs. Starting from an initial state  $\sigma$ , the parameterized circuit prepares a state  $\rho(\boldsymbol{\theta}) = W(\boldsymbol{\theta})\sigma W^\dagger(\boldsymbol{\theta})$ . A measurement operator  $O$  determines the cost function of the parameters

$\boldsymbol{\theta}$  via the expectation value with this state:

$$C(\boldsymbol{\theta}) = \text{Tr}[W(\boldsymbol{\theta})\sigma W^\dagger(\boldsymbol{\theta})O]. \quad (6)$$

A notable example, among many [6], is the variational quantum eigensolver [38], where the quantum states  $\sigma$  and  $\rho(\boldsymbol{\theta})$  represent electronic states of a molecule, and the measurement operator  $O$  is selected as the problem Hamiltonian. Thus, the cost function evaluates the energies of the prepared states, yielding (an approximation of) the electronic ground state when minimized.

QNN is a dominant model in quantum machine learning [39, 40]. QNNs can be viewed as a special case of VQAs, where data points are input as the initial states. As shown in Fig. 1, QNN can be defined using a data-based embedding  $U_{\mathbf{x}}$  for  $\mathbf{x} \in \mathcal{X}$  followed by variational embedding  $W(\boldsymbol{\theta})$  with  $m$  parameters  $\boldsymbol{\theta} \in [-\pi, \pi]^m$ . The most general cost function for QNNs can be defined as follows:

$$\begin{aligned} C(\boldsymbol{\theta}, \mathcal{X}) &= \sum_{i=1}^{N_s} c_i \text{Tr}[W(\boldsymbol{\theta})\rho(\mathbf{x}_i)W^\dagger(\boldsymbol{\theta})O] \\ &= \sum_{i=1}^{N_s} c_i \text{Tr}[W(\boldsymbol{\theta})U(\mathbf{x}_i)\rho_0 U^\dagger(\mathbf{x}_i)W^\dagger(\boldsymbol{\theta})O] = \sum_{i=1}^{N_s} c_i C(\boldsymbol{\theta}, \mathbf{x}_i) \end{aligned} \quad (7)$$

where  $O$  is a measurement operator.

BPs result from the concentration of the cost function with respect to variational parameters. Formally, one can define BPs in terms of the variance of the partial derivatives of the cost function.

**Definition 3. (Barren Plateaus).** The cost function defined for VQAs in Eq. (6) and QNNs in Eq. (7) exhibits a BP if the variance of the derivative of the cost function with respect to  $\theta_\mu \in \boldsymbol{\theta}$  decays exponentially with the number of qubits:

$$\text{Var}_{\boldsymbol{\theta}}[\partial_\mu C(\boldsymbol{\theta}, \mathbf{x}_i)] \leq F(n), \quad F(n) \in O(1/b^n) \quad (8)$$

BPs were first introduced in Ref. [12], where the source of the exponential suppression was identified to be the high expressivity of quantum circuits, which was termed as randomness-induced BP. Highly expressive circuits affect both gradient-free [41] and gradient-based [42] optimization approaches. Specifically, it was argued that random initialization of  $\boldsymbol{\theta}$  for a given  $W(\boldsymbol{\theta})$ , which forms a 2-design, leads to a BP [12, 43, 44]. Cerezo *et al.* [45] also studied BPs in shallow circuits and concluded that the quantum circuit with global measurement-based cost functions ( $O$  acting on all qubits) can suffer from BPs regardless of depth. Such BPs can be mitigated by utilizing local observables and shallow-depth circuits. However, this may eliminate the quantum advantage. BPs

have also been identified in the context of ML models based on tensor networks [46] and quantum circuits with high degree of entanglement [31].

BPs are closely related to narrow gorges in a cost function landscape formed when the volumetric fraction of the parameter space below a certain value is exponentially suppressed. Rigorously, cost concentration is defined according to Ref. [14] as follows.

**Definition 4. (Cost concentration & narrow gorges).** The cost function defined for VQAs in Eq. (6) and QNNs in Eq. (7) exhibits cost concentration if

$$\text{Var}_{\boldsymbol{\theta}_A}[\mathbb{E}_{\boldsymbol{\theta}}[C(\boldsymbol{\theta}, \mathbf{x}_i)] - C(\boldsymbol{\theta}_A, \mathbf{x}_i)] \leq G(n), \quad G(n) \in O(1/b^n), \quad b > 1. \quad (9)$$

Here,  $\boldsymbol{\theta}_A$  is a random draw from the uniform probability distribution over the parameter space. Furthermore, this cost function exhibits a narrow gorge if there exists a local minimum lower than the mean cost value by at least  $\delta(n) > 0$  with  $\delta(n) \in \Omega(1/\text{poly}(n))$ . The probability that the cost function value deviates from its mean by at least  $\delta$  at a randomly chosen point from a uniform distribution over the parameter space is bounded as follows:

$$\Pr_{\boldsymbol{\theta}_A}[|\mathbb{E}_{\boldsymbol{\theta}}[C(\boldsymbol{\theta}, \mathbf{x}_i)] - C(\boldsymbol{\theta}_A, \mathbf{x}_i)| \geq \delta] \leq \frac{G(n)}{\delta^2}, \quad G(n) \in O(1/b^n), \quad b > 1. \quad (10)$$

If a parametrized quantum circuit exhibits a BP then there exists cost concentration (and narrow gorges) satisfying the above condition and vice versa [14]. Hence, instead of considering gradients, one can study cost concentration. Note that the notation  $f(n) \in \mathcal{O}(g(n))$  and  $f(n) \in \Omega(g(n))$  specifies that  $f(n)$  is asymptotically bounded above and below by  $g(n)$ , respectively.

### III. BARREN PLATEAUS VS EXPONENTIAL CONCENTRATION

We relate EC in non-parametric (no trainable parameters) quantum kernels with the BP problem in both QNNs and general VQAs. Thus, we are concerned with the exponential concentration of the kernel function and, hence, kernel matrix elements. We first discuss a more straightforward case of QNN and then show how EC is related to BP in a general VQA. We begin by describing the kernel construction from the quantum circuits of QNN and VQA and subsequently prove that the quantum estimation of the kernel matrix, thus constructed, inherits the properties of the cost functions of QNN and VQA.

For a QNN, consider the cost function given by Eq. (7) with fixed  $\mathbf{x}_i$ . Following Eq. (9), we can write

$$\forall \mathbf{x}_i \in \mathcal{X}: \quad \text{Var}_{\boldsymbol{\theta}_A}[\mu_{\mathbf{x}_i} - C(\boldsymbol{\theta}_A, \mathbf{x}_i)] \leq F(n), \quad F(n) \in \mathcal{O}\left(\frac{1}{b^n}\right) \quad (11)$$

where  $\mu_{\mathbf{x}_i} = \mathbb{E}_{\boldsymbol{\theta}}[C(\boldsymbol{\theta}, \mathbf{x}_i)]$ . We propose the following construction of a quantum kernel: first, we match the variational part of the circuit  $W(\boldsymbol{\theta})$  with the data embedding  $U^\dagger(\mathbf{x}_i)$ <sup>1</sup>, and, second, we choose the measurement operator  $O$  to be the initial state  $\rho_0$ . In this way, we recover the state preparation  $\rho(\mathbf{x}) = W(\mathbf{x})\rho_0W^\dagger(\mathbf{x})$  for a data point  $\mathbf{x} \in \mathcal{X}$  through the variational part of the QNN. This leads to the quantum kernel in the form

$$\kappa(\mathbf{x}, \mathbf{x}') = \text{Tr}[W(\mathbf{x})\rho_0W^\dagger(\mathbf{x})W(\mathbf{x}')\rho_0W^\dagger(\mathbf{x}')]. \quad (12)$$

Alternatively, considering a general VQA with a cost function as in Eq. (6), one can construct a quantum kernel using the parametric quantum circuit of VQA as follows: first, insert the data points  $\mathbf{x}$  instead of the parameter vector  $\boldsymbol{\theta}$  in the parameterized circuit  $W(\mathbf{x})$ . This is more general than in the QNN setting due to the direct use of the variational ansatz  $W$  for the data encoding. Second, we note that either the initial state  $\sigma_0$  or the measurement operator  $O$  of the VQA must supply the encoding of the second data point  $\mathbf{x}'$ . Thus we can choose either  $\sigma = W(\mathbf{x}')\rho_0W^\dagger(\mathbf{x}')$  and  $O = \rho_0$  or  $\sigma = \rho_0$  and  $O = W^\dagger(\mathbf{x}')\rho_0W(\mathbf{x}')$ . While these two options may be considered equivalent with respect to the Schrödinger and Heisenberg pictures, it is common for BP theories to be formulated with different restrictions on the initial state and/or the measurement operator. We observe that the VQA cost function now implicitly relies on data encoded in either the initial state or the measurement operator, leading us to denote it as  $C(\boldsymbol{\theta}, \mathbf{x})$ , which is consistent with Eq. (7) for QNN. Note that by definition of the quantum (fidelity) kernel, we require global observables in the VQAs and QNNs.

We next relate exponential (polynomial) upper (lower) concentration bounds on the cost function to EC of the corresponding kernel matrices. To do this, we state the following lemmas with proofs provided in Appendix A 1.

**Lemma 1.** If there exists an upper bound under variation of the random variable  $\mathbf{x}_j$ ,

$$\forall \mathbf{x}_i: \quad \text{Var}_{\mathbf{x}_j} [f(\mathbf{x}_i, \mathbf{x}_j) \mid \mathbf{x}_i] \leq F(n) \quad (13)$$

with function  $f$  being symmetric in  $\mathbf{x}_i, \mathbf{x}_j$ , then this upper bound is doubled for the total variance:

$$\text{Var}_{\mathbf{x}_i, \mathbf{x}_j} [f(\mathbf{x}_i, \mathbf{x}_j)] \leq 2F(n) \quad (14)$$

**Lemma 2.** If there exists a lower bound under variation of the random variable  $\mathbf{x}_j$ ,

$$\forall \mathbf{x}_i: \quad \text{Var}_{\mathbf{x}_j} [f(\mathbf{x}_i, \mathbf{x}_j) \mid \mathbf{x}_i] \geq G(n) \quad (15)$$

---

<sup>1</sup> Without loss of generality, the data  $\mathcal{X}$  is assumed to be normalized and standardized to the range  $[-\pi, \pi]$ , which matches the typical range of parameters  $\boldsymbol{\theta}$ .



then this lower bound also applies to the total variance:

$$\text{Var}_{\mathbf{x}_i, \mathbf{x}_j} [f(\mathbf{x}_i, \mathbf{x}_j)] \geq G(n) \quad (16)$$

Given Lemmas 1 and 2, we state the theorem, which relates the bounds of the cost functions for VQAs and QNNs to the bounds for the corresponding quantum kernel, with a proof provided in Appendix A 2.

**Theorem 1.** Given a cost function, as defined either by Eq. (6) or Eq. (7), that satisfies either an asymptotic exponential upper bound (BP landscape) or polynomial lower bound (BP-free landscape), there exists a quantum kernel, whose variance with respect to data satisfies the same bounds. This quantum kernel is constructed using Eq. (12), which requires that the bounds remain applicable under the specified conditions for the VQA or QNN.

Formally, in the presence of a BP landscape, i.e.,

$$\exists F(n) \forall \mathbf{x}: \quad \text{Var}_{\boldsymbol{\theta}} [C(\boldsymbol{\theta}, \mathbf{x})] \leq F(n) \quad \text{with} \quad F(n) \in \mathcal{O}\left(\frac{1}{b^n}\right), \quad b > 1, \quad (17)$$

the corresponding quantum kernel (12) concentrates exponentially, i.e.

$$\text{Var}_{\mathbf{x}, \mathbf{x}'} [\kappa(\mathbf{x}, \mathbf{x}')] \leq 2F(n). \quad (18)$$

Vice versa, in the absence of a BP, i.e.,

$$\exists F(n) \forall \mathbf{x}: \quad \text{Var}_{\boldsymbol{\theta}} [C(\boldsymbol{\theta}, \mathbf{x})] \geq G(n) \quad \text{with} \quad G(n) \in \Omega\left(\frac{1}{\text{poly}(n)}\right), \quad (19)$$

the corresponding quantum kernel (12) does not concentrate exponentially

$$\text{Var}_{\mathbf{x}, \mathbf{x}'} [\kappa(\mathbf{x}, \mathbf{x}')] \geq G(n). \quad (20)$$

Consequently, for any VQA or QNN and corresponding quantum kernel within our framework, they either both suffer from BPs and EC or both are free from BPs and EC.

It should be mentioned that the choice of a state ( $O = \rho_0$ ) as the observable is uncommon in the literature on BPs, where observables are usually decomposed into Pauli operators [13, 34, 45]

$$O = \sum_{k=1}^p c_k \left( \bigotimes_{i=1}^n \sigma_i^{(k)} \right) \quad \text{with} \quad c_k \in \mathbb{R}, \quad \sigma_i^{(k)} \in \{I, X, Y, Z\}. \quad (21)$$

However, we note that computational basis states can also be expressed in the Pauli operator basis. For example, for a single qubit,  $|0\rangle\langle 0| = (I + Z)/2$ . This generalizes to  $n$  qubits via the tensor product as

$$\rho_0 = \sum_{\mathbf{b} \in \{0,1\}^n} \frac{1}{2^n} \bigotimes_{i=1}^n Z^{b_i} = O, \quad (22)$$

matching the form of Eq. (21).

#### IV. NUMERICAL DEMONSTRATION AND THEORETICAL EXAMPLES

To illustrate the results of Theorem 1, we construct a quantum kernel from permutation-invariant QNNs [34] utilizing the proposed framework. Theorem 1 predicts that this permutation-invariant quantum kernel does not exhibit EC. We illustrate this theoretical result with numerical examples and compare these kernel calculations with the initial demonstration of an exponentially concentrated quantum kernel presented in Fig. 2. We use Eq. (12) to construct a quantum kernel with the ansatz in Ref. [34] and evaluate the kernel matrices for the MNIST dataset considered before in Fig. 2. Figure 3 shows the kernel matrices thus obtained for different numbers of qubits  $n \in [5, 20]$ . The kernel matrix elements in Fig. 3 remain finite for large  $n$ , as opposed to the kernel matrices in Fig. 2 where the off-diagonal elements of the kernel matrices become negligible for  $n \leq 10$ . To provide a quantitative comparison between the results of Figs. 2 and 3, we compute the variance of  $k(\mathbf{x}_i, \mathbf{x}_j)$ . As shown in the right panel of Fig. 3,  $\text{Var}_{\mathbf{x}_i, \mathbf{x}_j}[k(\mathbf{x}_i, \mathbf{x}_j)]$  computed with the BP-free ansatz decreases only moderately as the number of qubits increases, while the ansatz used for the results in Fig. 2 leads to an exponential collapse of the variance magnitude.

Note that the present construction is not based on the principle of covariant quantum kernels [25]. Covariant quantum kernels assume that the data are induced by an underlying group structure. In contrast, the permutation-invariant quantum kernels, derived from permutation-invariant QNNs [34], assume data whose information in terms of interpretation and semantics remains unchanged under the action of the group. For instance, the data vectors  $\mathbf{x}$  may represent sets without any notion of order, i.e., any permutation of the components in  $\mathbf{x}$  has the same meaning. Hence, the data is invariant under permutations realized through the action of the symmetric group.

Finally, we state how our framework connects existing results from BPs in VQAs and EC in quantum kernels. In particular, BPs induced by ansatz expressivity [12] or global measurements [45] lead to concentration induced by expressivity and global measurements in quantum kernels, respectively, as established in Ref. [17]. More specifically, Ref. [12] assumes a setting in which the ansatz  $W(\boldsymbol{\theta})$  is expressive enough to establish a 2-design of the unitary group, resulting in a cost function (6) exhibiting BPs. Hence, using such an expressive ansatz to directly construct a quantum kernel via Eq. (12) must lead to exponential kernel concentration according to Theorem 1. Similarly, Ref. [45] considers a significantly shallow, such as of constant depth, and local 2-design ansatz. Due to the global measurement requirement, which is necessary to compute quantum kernels (fidelity), the emergence of BP on such global cost functions (6) is again transferred directly as exponential concentration in the corresponding quantum kernels (12) via Theorem 1.

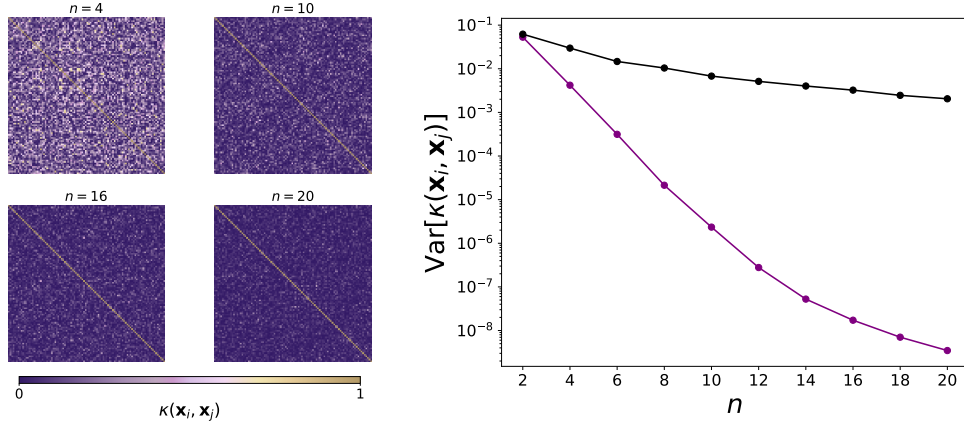


Figure 3. Kernel matrices computed with the BP-free ansatz [34] for binary classification on the MNIST dataset [37]. The matrices are constructed for 100 data points with the number of dimensions reduced to the corresponding number of qubits ( $n$ ) by principal component analysis. Each dimension is encoded into a single independent qubit. (Right) Variances of the kernel matrix elements computed with the BP-free ansatz (black) as a function of number of qubits in the range  $n \in [2, 20]$ . The depth of the circuit is equal to the number of qubits at each point. The purple line corresponds to the ansatz of Havlíček *et al.* [15] considered in Fig. 1. The depth of the circuit is kept constant.

## V. CONCLUSION

In summary, we have shown that a parameterized quantum circuit or a quantum neural network can be used to build a quantum kernel that inherits the concentration properties of the cost function of the corresponding VQA. More specifically, our results prove that the cost function concentration of a parametrized quantum circuit is equivalent to the concentration of the (non-parametric) kernel matrix. Our results imply that a VQA or QNN with a BP leads to quantum kernels that suffer from EC, whereas, more importantly, a BP-free VQA or QNN can be used to build a quantum kernel that does not exhibit exponential concentration. We have illustrated this by a numerical example with an ansatz that was previously shown to be BP-free. The present work implies that recently proposed algorithms for building BP-free quantum circuits can be applied to construct performant quantum kernels for machine learning.

However, it must be noted that constructing a quantum kernel from a BP-free VQA or QNN, which does not suffer from exponential concentration, does not guarantee that the resulting quantum kernel is practically useful or has an advantage over classical kernels. We base this statement on recent evidence indicating that the (provable) absence of BPs likely implies efficient classical simulability of the resulting quantum algorithm [47–49]. This is commonly referred to as *de-quantization*

of the quantum computing approach and makes the use of a quantum computer unnecessary. This previous work and the connection between BP and EC proven here suggest that quantum kernels that do not exhibit EC are likely efficiently simulable with classical hardware. Until a general BP-free construction with a provable quantum advantage is found, the present work should be interpreted to suggest that quantum fidelity kernels do not offer a quantum advantage, unless they encode inductive bias. This is consistent with the conclusion in Ref. [16] based on the analysis of the eigenspectra of quantum kernels. This suggests that the search for a quantum advantage of quantum kernel-based machine learning should focus on general strategies of encoding inductive bias.

### ACKNOWLEDGMENTS

This work was supported by the Natural Sciences and Engineering Research Council of Canada. We also acknowledge financial support from the Quantum Electronic Science & Technology (QuEST) Award given by the Stewart Blusson Quantum Matter Institute. We further acknowledge the NSERC CREATE in Quantum Computing Program, grant number 543245.

- 
- [1] Z. Krunić, F. F. Flöther, G. Seegan, N. D. Earnest-Noble, and O. Shehab, Quantum kernels for real-world predictions based on electronic health records, *IEEE Trans. Quantum Eng.* **3**, 1 (2022).
  - [2] E. Peters, J. Caldeira, A. Ho, S. Leichenauer, M. Mohseni, H. Neven, P. Spentzouris, D. Strain, and G. N. Perdue, Machine learning of high dimensional data on a noisy quantum processor, *Npj Quantum Inf.* **7**, 1 (2021).
  - [3] T. Hubregtsen, D. Wierichs, E. Gil-Fuster, P.-J. H. S. Derks, P. K. Faehrmann, and J. J. Meyer, Training quantum embedding kernels on near-term quantum computers, *Phys. Rev. A* **106**, 042431 (2022).
  - [4] M. Schuld and F. Petruccione, Quantum models as kernel methods, in *Machine Learning with Quantum Computers* (Springer International Publishing, Cham, 2021) pp. 217–245.
  - [5] M. Schuld and N. Killoran, Quantum machine learning in feature hilbert spaces, *Phys. Rev. Lett.* **122**, 040504 (2019).
  - [6] M. Cerezo, A. Arrasmith, R. Babbush, S. C. Benjamin, S. Endo, K. Fujii, J. R. McClean, K. Mitarai, X. Yuan, L. Cincio, and P. J. Coles, Variational quantum algorithms, *Nat. Rev. Phys.* **3**, 625 (2021).
  - [7] K. Bharti, A. Cervera-Lierta, T. H. Kyaw, T. Haug, S. Alperin-Lea, A. Anand, M. Degroote, H. Heimonen, J. S. Kottmann, T. Menke, W.-K. Mok, S. Sim, L.-C. Kwek, and A. Aspuru-Guzik, Noisy intermediate-scale quantum algorithms, *Rev. Mod. Phys.* **94**, 015004 (2022).

- [8] S. S. Gill, A. Kumar, H. Singh, M. Singh, K. Kaur, M. Usman, and R. Buyya, Quantum computing: A taxonomy, systematic review and future directions, *Softw. Pract. Exper.* **52**, 66 (2022).
- [9] S. Chen, J. Cotler, H.-Y. Huang, and J. Li, The complexity of nisq, *Nat. Commun.* **14**, 6001 (2023).
- [10] M. Cerezo, G. Verdon, H.-Y. Huang, L. Cincio, and P. J. Coles, Challenges and opportunities in quantum machine learning, *Nat. Comput. Sci.* **2**, 567 (2022).
- [11] J. Biamonte, P. Wittek, N. Pancotti, P. Rebentrost, N. Wiebe, and S. Lloyd, Quantum machine learning, *Nature* **549**, 195 (2017).
- [12] J. R. McClean, S. Boixo, V. N. Smelyanskiy, R. Babbush, and H. Neven, Barren plateaus in quantum neural network training landscapes, *Nat. Commun.* **9**, 4812 (2018).
- [13] M. Larocca, S. Thanasilp, S. Wang, K. Sharma, J. Biamonte, P. J. Coles, L. Cincio, J. R. McClean, Z. Holmes, and M. Cerezo, A review of barren plateaus in variational quantum computing, [arXiv:2405.00781](https://arxiv.org/abs/2405.00781) (2024).
- [14] A. Arrasmith, Z. Holmes, M. Cerezo, and P. J. Coles, Equivalence of quantum barren plateaus to cost concentration and narrow gorges, *Quantum Sci. Technol.* **7**, 045015 (2022).
- [15] V. Havlíček, A. D. Córcoles, K. Temme, A. W. Harrow, A. Kandala, J. M. Chow, and J. M. Gambetta, Supervised learning with quantum-enhanced feature spaces, *Nature* **567**, 209 (2019).
- [16] J. Kübler, S. Buchholz, and B. Schölkopf, The inductive bias of quantum kernels, *Adv. Neural Inf. Process. Syst.* **34**, 12661 (2021).
- [17] S. Thanasilp, S. Wang, M. Cerezo, and Z. Holmes, Exponential concentration in quantum kernel methods, *Nat. Commun.* **15**, 5200 (2024).
- [18] H.-K. Zhang, S. Liu, and S.-X. Zhang, Absence of barren plateaus in finite local-depth circuits with long-range entanglement, *Phys. Rev. Lett.* **132**, 150603 (2024).
- [19] Q. T. Nguyen, L. Schatzki, P. Braccia, M. Ragone, P. J. Coles, F. Sauvage, M. Larocca, and M. Cerezo, Theory for equivariant quantum neural networks, *PRX Quantum* **5**, 020328 (2024).
- [20] S. H. Sack, R. A. Medina, A. A. Michailidis, R. Kueng, and M. Serbyn, Avoiding barren plateaus using classical shadows, *PRX Quantum* **3**, 020365 (2022).
- [21] Z. Holmes, A. Arrasmith, B. Yan, P. J. Coles, A. Albrecht, and A. T. Sornborger, Barren plateaus preclude learning scramblers, *Phys. Rev. Lett.* **126**, 190501 (2021).
- [22] L. Friedrich and J. Maziero, Avoiding barren plateaus with classical deep neural networks, *Phys. Rev. A* **106**, 042433 (2022).
- [23] A. Kulshrestha and I. Safro, Beinit: Avoiding barren plateaus in variational quantum algorithms, in *QCE22* (2022) pp. 197–203.
- [24] M. Larocca, P. Czarnik, K. Sharma, G. Muraleedharan, P. J. Coles, and M. Cerezo, Diagnosing Barren Plateaus with Tools from Quantum Optimal Control, *Quantum* **6**, 824 (2022).
- [25] J. R. Glick, T. P. Gujarati, A. D. Córcoles, Y. Kim, A. Kandala, J. M. Gambetta, and K. Temme, Covariant quantum kernels for data with group structure, *Nat. Phys.* **20**, 479 (2024).
- [26] R. Shaydulin and S. M. Wild, Importance of kernel bandwidth in quantum machine learning, *Phys.*

- [Rev. A \*\*106\*\*, 042407 \(2022\)](#).
- [27] Y. Suzuki, H. Kawaguchi, and N. Yamamoto, [Quantum Fisher kernel for mitigating the vanishing similarity issue](#) (2022).
- [28] H.-Y. Huang, M. Broughton, M. Mohseni, R. Babbush, S. Boixo, H. Neven, and J. R. McClean, Power of data in quantum machine learning, [Nat. Commun. \*\*12\*\*, 2631 \(2021\)](#).
- [29] S. Wang, E. Fontana, M. Cerezo, K. Sharma, A. Sone, L. Cincio, and P. J. Coles, Noise-induced barren plateaus in variational quantum algorithms, [Nat. Commun. \*\*12\*\*, 6961 \(2021\)](#).
- [30] Z. Holmes, K. Sharma, M. Cerezo, and P. J. Coles, Connecting ansatz expressibility to gradient magnitudes and barren plateaus, [PRX Quantum \*\*3\*\*, 010313 \(2022\)](#).
- [31] C. Ortiz Marrero, M. Kieferová, and N. Wiebe, Entanglement-induced barren plateaus, [PRX Quantum \*\*2\*\*, 040316 \(2021\)](#).
- [32] A. V. Uvarov and J. D. Biamonte, On barren plateaus and cost function locality in variational quantum algorithms, [J. Phys. A: Math. Theor. \*\*54\*\*, 245301 \(2021\)](#).
- [33] N. Innan, M. Khan, B. Panda, and M. Bennai, Enhancing quantum support vector machines through variational kernel training, [Quantum Inf. Process. \*\*22\*\*, 374 \(2023\)](#).
- [34] L. Schatzki, M. Larocca, Q. T. Nguyen, F. Sauvage, and M. Cerezo, Theoretical guarantees for permutation-equivariant quantum neural networks, [Npj Quantum Inf. \*\*10\*\*, 12 \(2024\)](#).
- [35] M. Schuld and F. Petruccione, *Machine learning with quantum computers*, 2nd ed., Quantum Science and Technology (Springer Nature, Cham, Switzerland, 2021).
- [36] A. Canatar, B. Bordelon, and C. Pehlevan, Spectral bias and task-model alignment explain generalization in kernel regression and infinitely wide neural networks, [Nat. Commun. \*\*12\*\*, 2914 \(2021\)](#).
- [37] L. Deng, The mnist database of handwritten digit images for machine learning research [best of the web], [IEEE Signal Process. Mag. \*\*29\*\*, 141 \(2012\)](#).
- [38] A. Peruzzo, J. McClean, P. Shadbolt, M.-H. Yung, X.-Q. Zhou, P. J. Love, A. Aspuru-Guzik, and J. L. O'Brien, A variational eigenvalue solver on a photonic quantum processor, [Nat. Commun. \*\*5\*\*, 4213 \(2014\)](#).
- [39] K. Beer, D. Bondarenko, T. Farrelly, T. J. Osborne, R. Salzmann, D. Scheiermann, and R. Wolf, Training deep quantum neural networks, [Nat. Commun. \*\*11\*\*, 808 \(2020\)](#).
- [40] S. K. Jeswal and S. Chakraverty, Recent Developments and Applications in Quantum Neural Network: A Review, [Arch. Comput. Methods Eng. \*\*26\*\*, 793 \(2019\)](#).
- [41] A. Arrasmith, M. Cerezo, P. Czarnik, L. Cincio, and P. J. Coles, Effect of barren plateaus on gradient-free optimization, [Quantum \*\*5\*\*, 558 \(2021\)](#).
- [42] M. Cerezo and P. J. Coles, Higher order derivatives of quantum neural networks with barren plateaus, [Quantum Sci. Technol. \*\*6\*\*, 035006 \(2021\)](#).
- [43] F. G. S. L. Brandão, A. W. Harrow, and M. Horodecki, Local random quantum circuits are approximate polynomial-designs, [Commun. Math. Phys. \*\*346\*\*, 397 \(2016\)](#).
- [44] C. Dankert, R. Cleve, J. Emerson, and E. Livine, Exact and approximate unitary 2-designs and their

- application to fidelity estimation, *Phys. Rev. A* **80**, 012304 (2009).
- [45] M. Cerezo, A. Sone, T. Volkoff, L. Cincio, and P. J. Coles, Cost function dependent barren plateaus in shallow parametrized quantum circuits, *Nat. Commun.* **12**, 1791 (2021).
- [46] Z. Liu, L.-W. Yu, L.-M. Duan, and D.-L. Deng, Presence and absence of barren plateaus in tensor-network based machine learning, *Phys. Rev. Lett.* **129**, 270501 (2022).
- [47] M. Cerezo, M. Larocca, D. García-Martín, N. L. Diaz, P. Braccia, E. Fontana, M. S. Rudolph, P. Bermejo, A. Ijaz, S. Thanasilp, E. R. Anschuetz, and Z. Holmes, Does provable absence of barren plateaus imply classical simulability? (2023).
- [48] L. Leone, S. F. E. Oliviero, L. Cincio, and M. Cerezo, [On the practical usefulness of the Hardware Efficient Ansatz](#) (2022).
- [49] A. Basheer, Y. Feng, C. Ferrie, and S. Li, [Alternating layered variational quantum circuits can be classically optimized efficiently using classical shadows](#) (2022).
- [50] M. J. Schervish and M. H. DeGroot, *Probability and statistics*, Vol. 563 (Pearson Education London, UK, 2014).

## Appendix A: Proofs

This appendix presents the proofs for the two lemmas and the main theorem of this work.

### 1. Proofs of lemmas

**Lemma 1** (*restated*). If there exists an upper bound under variation of the random variable  $\mathbf{x}_j$ ,

$$\forall \mathbf{x}_i: \quad \text{Var}_{\mathbf{x}_j} [f(\mathbf{x}_i, \mathbf{x}_j) \mid \mathbf{x}_i] \leq F(n) \quad (\text{A1})$$

with function  $f$  being symmetric in  $\mathbf{x}_i, \mathbf{x}_j$ , then this upper bound is doubled for the total variance:

$$\text{Var}_{\mathbf{x}_i, \mathbf{x}_j} [f(\mathbf{x}_i, \mathbf{x}_j)] \leq 2F(n) \quad (\text{A2})$$

*Proof.* The law of total variance provides the following decomposition

$$\text{Var}_{\mathbf{x}_i, \mathbf{x}_j} [f(\mathbf{x}_i, \mathbf{x}_j)] = \mathbb{E}_{\mathbf{x}_i} [\text{Var}_{\mathbf{x}_j} [f(\mathbf{x}_i, \mathbf{x}_j) \mid \mathbf{x}_i]] + \text{Var}_{\mathbf{x}_i} [\mathbb{E}_{\mathbf{x}_j} [f(\mathbf{x}_i, \mathbf{x}_j) \mid \mathbf{x}_i]], \quad (\text{A3})$$

where both terms are each upper bounded by  $F(n)$ . The bound on the first term trivially follows from the lemma's condition, and for the second term we decompose the variance into covariances [50]

$$\text{Var}_{\mathbf{x}_i} [\mathbb{E}_{\mathbf{x}_j} [f(\mathbf{x}_i, \mathbf{x}_j) \mid \mathbf{x}_i]] = \text{Var}_{\mathbf{x}_i} \left[ \int_{\mathcal{X}} p(\mathbf{x}'_j \mid \mathbf{x}_i) f(\mathbf{x}_i, \mathbf{x}'_j) d\mathbf{x}'_j \right] \quad (\text{A4})$$

$$= \int_{\mathcal{X}} \int_{\mathcal{X}} p(\mathbf{x}'_j \mid \mathbf{x}_i) p(\mathbf{x}''_j \mid \mathbf{x}_i) \text{Cov}[f(\mathbf{x}_i, \mathbf{x}'_j), f(\mathbf{x}_i, \mathbf{x}''_j)] d\mathbf{x}'_j d\mathbf{x}''_j, \quad (\text{A5})$$

where the primes indicate realizations  $\mathbf{x}'_j \in \mathcal{X}$  of the random variables  $\mathbf{x}_j$  over  $\mathcal{X}$ . The Cauchy-Schwarz inequality provides the upper bounds on the covariances [50]

$$\sqrt{\text{Var}_{\mathbf{x}_i} [f(\mathbf{x}_i, \mathbf{x}'_j) \mid \mathbf{x}'_j] \text{Var}_{\mathbf{x}_i} [f(\mathbf{x}_i, \mathbf{x}''_j) \mid \mathbf{x}''_j]},$$

which, in turn, are upper bounded by  $F(n)$  as per the lemma's condition and the symmetry of function  $f$  in its arguments. Since  $F(n)$  exists independently of realizations  $\mathbf{x}'_j, \mathbf{x}''_j$ , the integrals trivially simplify, which concludes the proof by applying the derived bounds to Eq. (A3):

$$\text{Var}_{\mathbf{x}_i, \mathbf{x}_j} [f(\mathbf{x}_i, \mathbf{x}_j)] = \mathbb{E}_{\mathbf{x}_i} [\text{Var}_{\mathbf{x}_j} [f(\mathbf{x}_i, \mathbf{x}_j) \mid \mathbf{x}_i]] + \text{Var}_{\mathbf{x}_i} [\mathbb{E}_{\mathbf{x}_j} [f(\mathbf{x}_i, \mathbf{x}_j) \mid \mathbf{x}_i]] \quad (\text{A6})$$

$$\leq F(n) + F(n) \quad (\text{A7})$$

$$= 2F(n) \quad (\text{A8})$$

□



**Lemma 2 (restated).** If there exists a lower bound under variation of the random variable  $\mathbf{x}_j$ ,

$$\forall \mathbf{x}_i: \quad \text{Var}_{\mathbf{x}_j} [f(\mathbf{x}_i, \mathbf{x}_j) \mid \mathbf{x}_i] \geq G(n) \quad (\text{A9})$$

then this lower bound also holds for the total variance:

$$\text{Var}_{\mathbf{x}_i, \mathbf{x}_j} [f(\mathbf{x}_i, \mathbf{x}_j)] \geq G(n) \quad (\text{A10})$$

*Proof.*

$$\text{Var}_{\mathbf{x}_i, \mathbf{x}_j} [f(\mathbf{x}_i, \mathbf{x}_j)] = \mathbb{E}_{\mathbf{x}_i, \mathbf{x}_j} [f(\mathbf{x}_i, \mathbf{x}_j)^2] - \mathbb{E}_{\mathbf{x}_i, \mathbf{x}_j} [f(\mathbf{x}_i, \mathbf{x}_j)]^2 \quad (\text{A11})$$

$$= \mathbb{E}_{\mathbf{x}_i} \left[ \mathbb{E}_{\mathbf{x}_j} [f(\mathbf{x}_i, \mathbf{x}_j)^2 \mid \mathbf{x}_i] \right] - \mathbb{E}_{\mathbf{x}_i} \left[ \mathbb{E}_{\mathbf{x}_j} [f(\mathbf{x}_i, \mathbf{x}_j) \mid \mathbf{x}_i] \right]^2 \quad (\text{A12})$$

$$\geq \mathbb{E}_{\mathbf{x}_i} \left[ \mathbb{E}_{\mathbf{x}_j} [f(\mathbf{x}_i, \mathbf{x}_j)^2 \mid \mathbf{x}_i] \right] - \mathbb{E}_{\mathbf{x}_i} \left[ \mathbb{E}_{\mathbf{x}_j} [f(\mathbf{x}_i, \mathbf{x}_j) \mid \mathbf{x}_i]^2 \right] \quad (\text{A13})$$

$$= \mathbb{E}_{\mathbf{x}_i} \left[ \mathbb{E}_{\mathbf{x}_j} [f(\mathbf{x}_i, \mathbf{x}_j)^2 \mid \mathbf{x}_i] - \mathbb{E}_{\mathbf{x}_j} [f(\mathbf{x}_i, \mathbf{x}_j) \mid \mathbf{x}_i]^2 \right] \quad (\text{A14})$$

$$= \mathbb{E}_{\mathbf{x}_i} [\text{Var}_{\mathbf{x}_j} [f(\mathbf{x}_i, \mathbf{x}_j) \mid \mathbf{x}_i]] \quad (\text{A15})$$

$$\geq \mathbb{E}_{\mathbf{x}_i} [G(n)] = G(n). \quad (\text{A16})$$

We use: the law of total expectation in Eq. (A12) and Jensen's inequality, which states that the convex transformation of a mean is less than or equal to the mean applied after convex transformation, in Eq. (A13) as  $x \mapsto x^2$  is a convex function. We also use linearity of expectation.  $\square$

## 2. Proof of main theorem

**Theorem 1 (restated).** Given a cost function, as defined either by Eq. (6) or Eq. (7), that satisfies either an asymptotic exponential upper bound (BP landscape) or polynomial lower bound (BP-free landscape), there exists a quantum kernel, whose variance with respect to data satisfies the same bounds. This quantum kernel is constructed using Eq. (12) that imposes conditions on VQA and QNN. These conditions are explicitly specified in Appendix A 1.

Formally, in the presence of a BP landscape, i.e.,

$$\exists F(n) \forall \mathbf{x}: \quad \text{Var}_{\boldsymbol{\theta}} [C(\boldsymbol{\theta}, \mathbf{x})] \leq F(n) \quad \text{with} \quad F(n) \in \mathcal{O} \left( \frac{1}{b^n} \right), \quad b > 1, \quad (\text{A17})$$

the corresponding quantum kernel (12) concentrates exponentially

$$\text{Var}_{\mathbf{x}, \mathbf{x}'} [\kappa(\mathbf{x}, \mathbf{x}')] \leq 2F(n). \quad (\text{A18})$$

Vice versa, in the absence of a BP, i.e.,

$$\exists F(n) \forall \mathbf{x}: \quad \text{Var}_{\boldsymbol{\theta}} [C(\boldsymbol{\theta}, \mathbf{x})] \geq G(n) \quad \text{with} \quad G(n) \in \Omega \left( \frac{1}{\text{poly}(n)} \right), \quad (\text{A19})$$

the corresponding quantum kernel (12) does not concentrate exponentially

$$\text{Var}_{\mathbf{x}, \mathbf{x}'} [\kappa(\mathbf{x}, \mathbf{x}')] \geq G(n). \quad (\text{A20})$$

*Proof.* The theorem assumes our construction introduced in the main text in Sec. III, summarized in the following conditions for a QNN:

- same ansatz is chosen for the variational part of the QNN as for data embedding in the quantum kernel  $U(\mathbf{x}) \leftrightarrow W^\dagger(\mathbf{x})$ ;
- The initial state also serves as the observable  $O = \rho_0$ .

For a general VQA, the conditions are as follows:

- The parameter vector  $\boldsymbol{\theta}$  in the quantum circuit  $W(\mathbf{x})$  is replaced by the (first) data point  $\mathbf{x}$
- Either the initial state  $\sigma_0$  or the measurement operator  $O$  provides the encoding of the second data point  $\mathbf{x}'$ :  $\sigma = W(\mathbf{x}')\rho_0W^\dagger(\mathbf{x}')$  and  $O = \rho_0$ , or  $\sigma = \rho_0$  and  $O = W^\dagger(\mathbf{x}')\rho_0W(\mathbf{x}')$

Under these conditions and upon substitution  $\boldsymbol{\theta} \rightarrow \mathbf{x}_j$  in the QNN case, Eq. (12) applies, i.e., we recover the quantum kernel formulation. Then, Eq. (17) yields

$$\forall \mathbf{x}_i: \quad \text{Var}_{\mathbf{x}_j} [\kappa(\mathbf{x}_i, \mathbf{x}_j) \mid \mathbf{x}_i] \in \mathcal{O}\left(\frac{1}{b^n}\right), \quad b > 1. \quad (\text{A21})$$

Conversely, if no BPs exist Eq. (19) implies a lower bound on the variance

$$\forall \mathbf{x}_i: \quad \text{Var}_{\mathbf{x}_j} [\kappa(\mathbf{x}_i, \mathbf{x}_j) \mid \mathbf{x}_i] \in \Omega\left(\frac{1}{\text{poly}(n)}\right). \quad (\text{A22})$$

Additionally, recall that by definition, the kernel function is symmetric in its arguments, i.e.,  $\kappa(\mathbf{x}_i, \mathbf{x}_j) = \kappa(\mathbf{x}_j, \mathbf{x}_i)$ . It directly follows from Lemmas 1 and 2 that these asymptotic bounds also apply to the total variance (where constant factors are absorbed asymptotically)

$$\text{Var}_{\mathbf{x}_j, \mathbf{x}_i} [\kappa(\mathbf{x}_i, \mathbf{x}_j)] \in \mathcal{O}\left(\frac{1}{b^n}\right) \quad \text{with } b > 1 \quad \text{and} \quad (\text{A23})$$

$$\text{Var}_{\mathbf{x}_j, \mathbf{x}_i} [\kappa(\mathbf{x}_i, \mathbf{x}_j)] \in \Omega\left(\frac{1}{\text{poly}(n)}\right), \quad (\text{A24})$$

which concludes the proof.  $\square$